Acta Crystallographica Section D
Biological Crystallography
ISSN 0907-4449

Overproduction, crystallization and preliminary X-ray diffraction analysis of a quinone oxidoreductase from *Thermus thermophilus* HB8

Yoshimitsu Shimomura,[a] Kazuko Sumiguchi-Agari,[b] Ryoji Masui,[a,b] Seiki Kuramitsu[a,b] and Keiichi Fukuyama[a,b]*

[a]Department of Biology, Graduate School of Science, Osaka University, Toyonaka, Osaka 560-0043, Japan, and [b]RIKEN Harima Institute/SPring-8, 1-1-1 Koto, Mikazuki-cho, Sayo-gun, Hyogo 679-5148, Japan

Correspondence e-mail: fukuyama@bio.sci.osaka-u.ac.jp

Received 4 April 2002
Accepted 5 June 2002

A probable quinone oxidoreductase (MW = 32.1 kDa) from *Thermus thermophilus* HB8 was overproduced in *Escherichia coli* and purified. Gel-filtration chromatography suggested the protein to be in a dimeric state. This protein enhanced the reduction activity of quinones by NADPH. It was crystallized in the absence and the presence of NADPH by the hanging-drop vapour-diffusion method. Both crystals were hexagonal, space group $P6_122$ or $P6_522$, with unit-cell parameters $a = b = 77.6$, $c = 236.7$ Å for the apo form and $a = b = 77.6$, $c = 235.9$ Å for the complex with NADPH. They diffract to better than 2.3 Å resolution with synchrotron radiation. The asymmetric unit has one protein subunit ($V_M = 3.2$ Å^3 Da^{-1} and $V_{sol} = 0.62$ for the apo form), indicating that the twofold axis of the dimeric protein and the crystallographic twofold axis coincide.

1. Introduction

Quinone oxidoreductases are mainly classified into two types, membrane-bound and soluble. Membrane-bound NADH quinone oxidoreductases function in the respiratory chain of bacteria and the mitochondria of eukaryotes (Yagi, 1991). These enzymes have complex forms consisting of multiple subunits and bear such cofactors as FMN, FAD and iron–sulfur clusters. In contrast, soluble quinone oxidoreductases are single-polypeptide enzymes that are divided into two types represented by DT-diaphorase and ζ-crystallin. DT-diaphorase, a widely distributed protein, catalyzes NAD(P)H-dependent two-electron reduction of quinone substrates and bears FAD (Chen *et al.*, 2000). DT-diaphorases may protect cells from the toxic effects of quinones (Chen *et al.*, 2000). ζ-Crystallin is a major eye-lens protein in guinea pigs, camels and other vertebrates (Rao *et al.*, 1992). It does not require FMN, FAD or iron–sulfur clusters and reduces substrate quinones by a NAD(P)H-dependent one-electron-transfer process that produces a semiquinone radical which causes generation of H_2O_2 (Rao *et al.*, 1992). The physiological function of this enzyme is unknown, but it may have a metabolic role or detoxify quinones (Tumminia *et al.*, 1993).

During the sequencing and characterization of genes in the genome of the Gram-negative eubacterium *Thermus thermophilus* HB8 (Yokoyama *et al.*, 2000), we found an open reading frame (ORF) which is homologous to ζ-crystallin-type quinone oxidoreductases rather than DT-diaphorases. The sequence of this ORF shares a marginal sequence identity (∼20%) with that of the quinone oxidoreductase from *Escherichia coli* (ecQOR). The crystal structure of ecQOR in complex with NADPH (Thorn *et al.*, 1995) shows that this enzyme has a fold belonging to the medium-chain dehydrogenase/reductase (MDR) superfamily (Persson *et al.*, 1994), which consists of such enzymes as horse liver alcohol dehydrogenase (LADH; Eklund *et al.*, 1976) and glucose dehydrogenase (GDH; John *et al.*, 1994), although ecQOR has very low sequence identity with LADH and GDH. The proteins in the MDR superfamily have NAD(P)H-dependent dehydrogenase or reductase activities and consist of nucleotide-binding and catalytic domains. The nucleotide-binding domain has the G*X*G*XX*G sequence as its typical nucleotide-binding motif, but the sequence is modified in some enzymes: LADH, G*X*G*XX*G; GDH, G*X*G*XX*A; ζ-crystallin, G*XX*G*XX*G; ecQOR, A*XX*G*XX*G (Edwards *et al.*, 1996). The product of the ORF from *T. thermophilus* is a 32 kDa protein consisting of 302 amino-acid residues. It has the same A*XX*G*XX*G fingerprint motif as ecQOR, but unlike LADH or GDH it has no zinc-binding residue. Therefore, this protein is considered to be similar to ecQOR both in sequence homology and its functional features; we have therefore named it putative quinone oxidoreductase (ttQOR).

We overeproduced the putative ttQOR in *E. coli* and it was characterized by the fact that it reduces quinones in the presence of NADPH. Conformation of its active-site residues and change on cofactor binding are

important for understanding both its enzymatic activity and cofactor recognition (Cobessi *et al.*, 1999); the crystal structure of ecQOR is only known in complex with NADPH (Thorn *et al.*, 1995). To clarify the mechanisms of nucleotide binding and enzyme action, we performed crystallographic analyses of the enzyme in the absence and presence of NADPH. Here, we report the crystallization and preliminary X-ray analysis of ttQOR in the apo form and in complex with NADPH.

2. Materials and methods

2.1. Cloning, sequencing and overproduction

Using the DNA sequence (DDBJ/EMBL/GenBank accession No. AB085185; project code 0379) homologous to the NADPH quinone oxidoreductase found in the *T. thermophilus* HB8 genome, we synthesized two primers for amplification of the target gene by a polymerase chain reaction: 5′-ATAT**CATATG**AAAGCCTGGGTGACCTGAAGCGGCTTGGCG-3′ and 5′-ATAT**AGATCT**TTATTAGAGCCGCACCACCACCTTCCCCGTG-3′, in which the *Nde*I and *Bgl*II sites, respectively, are in bold. Amplification was performed by the standard protocols and the amplified gene fragment ligated into pT7Blue (Novagen) by TA cloning. Using the *Nde*I and *Bam*HI sites, the fragment bearing the target gene was ligated into pET-11a (Novagen) and the expression plasmid used to transform the *E. coli* strain BL21(DE3) (Novagen). The transformant was cultured at 310 K in 6 l of Luria broth supplemented with ampicillin (50 µg ml^{-1}). Cells were harvested by centrifugation after 16 h and stored at 193 K until use.

2.2. Protein purification

Unless otherwise noted, protein was purified at room temperature. Frozen cells were thawed, suspended in 20 m*M* Tris–HCl pH 8.0, 5 m*M* 2-mercaptoethanol and 50 m*M* NaCl and then disrupted by sonication. The cell lysate was incubated at 343 K for 10 min, kept on ice for 12 min and then ultracentrifuged (200 000*g*) for 60 min at 277 K. Ammonium sulfate was added to the resulting supernatant to 25% saturation, after which the solution was applied to a Resource ISO column (Amersham Pharmacia Biotech) equilibrated with 50 m*M* sodium phosphate pH 7.0 containing 25% saturated ammonium sulfate. Protein was eluted with a linear gradient of ammonium sulfate of 25–0% saturation in 50 m*M* sodium phosphate. Fractions containing the target protein were collected, desalted by dialysis and applied in 20 m*M* Tris–HCl pH 8.0 to a Resource Q column (Amersham Pharmacia Biotech); protein was eluted with a linear gradient of 0–500 m*M* NaCl in the same buffer. Fractions containing the target protein were desalted and applied to a hydroxyapatite column CHT2-I (Bio-Rad) previously equilibrated with 10 m*M* sodium phosphate pH 7.0. Protein was eluted with a linear gradient of 10–250 m*M* sodium phosphate. Fractions containing the target protein then were loaded onto a HiLoad 16/60 Superdex 75pg column (Amersham Pharmacia Biotech) equilibrated with 20 m*M* Tris–HCl pH 8.0 and 150 m*M* NaCl and eluted with the same buffer. After the addition of 1 m*M* dithiothreitol, the peak fractions were concentrated and stored at 277 K. At each step, the fractions were analyzed by SDS–PAGE with 12%(*w*/*v*) acrylamide gel.

2.3. Characterization of the protein

The oligomeric state of ttQOR in solution was estimated at 277 K by gel-filtration chromatography. ttQOR (1 ml at 1 mg ml^{-1}) was loaded onto a HiPrep 16/60 Sephacryl S-200 High Resolution column using AKTA explorer 10S (Amersham Pharmacia Biotech) and then eluted with 150 m*M* NaCl, 20 m*M* Tris–HCl pH 8.0 at a flow rate of 0.3 ml min^{-1}. The calibration curve was obtained by the use of molecular-weight markers (Sigma).

The NADPH-dependent *p*-benzoquinone reduction activity of ttQOR was measured by monitoring the decrease in absorbance of NADPH at 340 nm (Rao *et al.*, 1992). The reaction solution contained 0.1 *M* Tris–HCl pH 7.8, 0.2 m*M* EDTA, 0.1 m*M* NADPH and 0.25 or 1.25 µ*M* ttQOR. *p*-Benzoquinone dissolved in ethanol was added to 1 ml of the mixture to start the reaction. The final ethanol concentration was less than 1%. Absorbance at 340 nm was monitored for 5 min in a UV-3101PC UV–Vis NIR scanning spectrophotometer (Shimadzu) at room temperature.

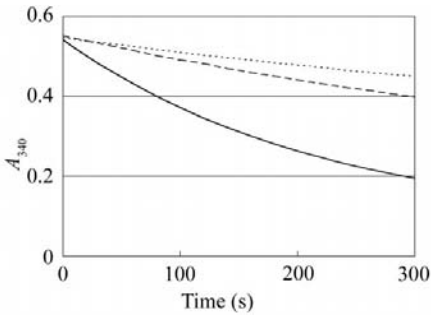

Figure 1
Enzyme-activity assay. Measurement conditions are described in the text. Dotted line, 0 µ*M* ttQOR, 250 µ*M* *p*-benzoquinone; broken line, 0.25 µ*M* ttQOR, 250 µ*M* *p*-benzoquinone; solid line, 1.25 µ*M* ttQOR, 250 µ*M* *p*-benzoquinone.

2.4. Crystallization

Crystallization conditions for apo-ttQOR were surveyed using the hanging-drop vapour-diffusion method with Crystal Screen Kits (Hampton Research) at 293 K. The initial protein concentration was 8.4 mg ml^{-1} in 20 m*M* Tris–HCl pH 8.0, 150 m*M* NaCl and 1 m*M* DTT. Drops were prepared by mixing 1 µl of the protein solution with 1 µl of the reservoir solution and were equilibrated against the reservoir solution. Co-crystallization trials with NADPH were set up in the same way, where the initial protein and NADPH concentrations were 21 mg ml^{-1} and 14 m*M*, respectively.

2.5. X-ray diffraction analysis

Crystals were soaked for a few seconds in Paratone-N (Hampton Research), which served as a cryoprotectant. Each crystal was mounted on a cryoloop and then flash-

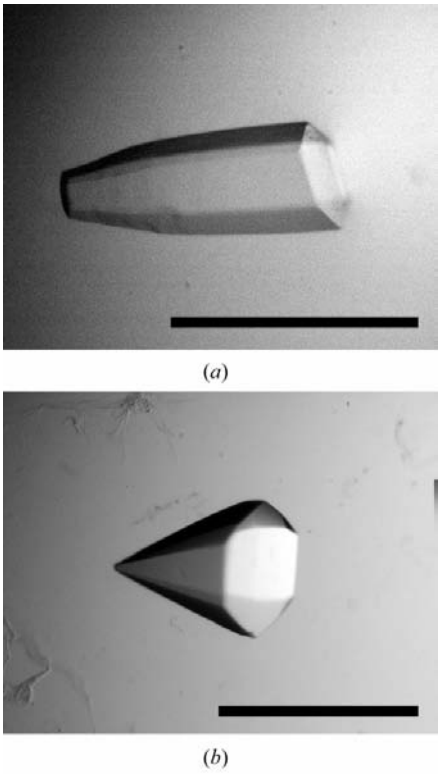

(*a*)

(*b*)

Figure 2
(*a*) Hexagonal crystal of ttQOR (apo form) from *T. thermophilus* HB8. (*b*) Crystal of ttQOR in complex with NADPH. The scale bars represent 0.5 mm.

Table 1
Crystal data and diffraction measurement results.

Values in parentheses are for the outermost shell (2.51–2.38 Å).

	Apo form	Complex with NADPH
Space group	$P6_122$ or $P6_522$	$P6_122$ or $P6_522$
Unit-cell parameters (Å)	$a = b = 77.6$, $c = 236.7$	$a = b = 77.6$, $c = 235.9$
No. measured reflections	62242 (9133)	249653 (31965)
No. unique reflections	15080 (2156)	17588 (2430)
Resolution range (Å)	58.7–2.38	67.4–2.38
$R_{\rm merge}$† (%)	9.3 (16.6)	6.6 (11.9)
Completeness (%)	86.4 (85.7)	98.8 (97.1)
Mean $I/\sigma(I)$	5.1 (3.9)	7.7 (5.3)

† $R_{\rm merge} = \sum_h \sum_i |I_i(h) - \langle I(h)\rangle| / \sum_h \sum_i I_i(h)$, where $\langle I(h)\rangle$ is the average intensity over equivalent reflections.

cooled in cryostream at 103 K. X-ray diffraction data were collected with a MAR CCD using synchrotron radiation at BL44B2, SPring-8. The oscillation angle was 1.0°, the exposure time was 40 s per frame and the camera distance was 180 mm. Diffraction images were processed using *MOSFLM* (Leslie, 1992) and the *CCP*4 program suite (Collaborative Computational Project, Number 4, 1994).

3. Results and discussion

ttQOR was purified to homogeneity as judged by SDS–PAGE. The final amount of purified protein was 38 mg and the yield was 2 mg of protein per gram of cells. In the gel filtration, ttQOR eluted at a retention time corresponding to about 52 kDa, which suggests that ttQOR exists as dimer in solution. Results of the enzyme-activity assay are shown in Fig. 1. The decrease in absorbance at 340 nm in the reaction in the presence of ttQOR was more rapid than that in its absence, showing that ttQOR catalyzed NADPH-dependent *p*-benzoquinone reduction.

Hexagonal crystals of ttQOR were obtained by the use of Crystal Screen 2 No. 42 solution (12% glycerol, 0.1 *M* Tris pH 8.5, 1.5 *M* ammonium sulfate) (Fig. 2). Crystal dimensions were about 0.2 × 0.2 × 0.5 mm. When NADPH was present in the drops, crystals were grown with Crystal Screen No. 3 solution (0.4 *M* ammonium dihydrogen phosphate). The crystal shape was similar to that of crystals grown in the absence of NADPH.

ttQOR crystals grown in the absence and presence of NADPH belong to the hexagonal space group $P6_122$ or $P6_522$. Unit-cell parameters are $a = b = 77.6$, $c = 236.7$ Å for the apo form and $a = b = 77.6$, $c = 235.9$ Å for the complex with NADPH (Table 1). Both types of crystals diffract to better than 2.3 Å resolution with synchrotron radiation (Fig. 3). When the asymmetric unit contains one ttQOR subunit, the respective $V_{\rm M}$ and $V_{\rm sol}$ values (Matthews, 1968) are 3.2 Å^3 Da^{-1} and 0.62 for the apo form, indicating that the dimeric protein twofold axis coincides with the crystallographic twofold axis. As seen in Fig. 3, diffraction spots along the c^* axis were so close together that synchrotron radiation was required to resolve the individual spots. Results of the preliminary X-ray intensity measurements are given in Table 1. We now aim to solve the structure by the MAD technique with selenium as the anomalous scattering atom. ttQOR contains five methionine residues. Preparation of the SeMet derivative of ttQOR and its crystallization are in progress.

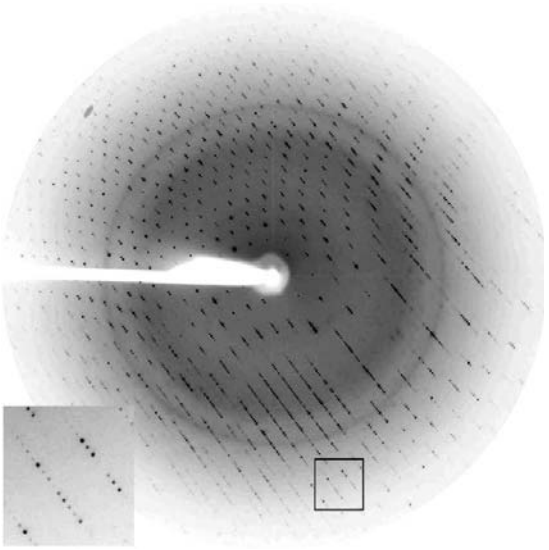

Figure 3
Diffraction pattern of the ttQOR crystal. The frame edge is at 2.38 Å resolution.

We thank Dr Taiji Matsu of the RIKEN Harima Institute for his help with data collection using synchrotron radiation at the BL44B2 of SPring-8 and Dr Yoshimitsu Kakuta for his valuable suggestions. This work was supported in part by a Grant-in-Aid for Scientific Research on a Priority Area (Biological Machinery No. 11169223) to KF from the Ministry of Education, Culture, Sports, Science and Technology of Japan.

References

Chen, S., Wu, K. & Knox, R. (2000). *Free Radic. Biol. Med.* **29**, 276–284.
Cobessi, D., Tete-Favier, F., Marchal, S., Azza, S., Branlant, G. & Aubry, A. (1999). *J. Mol. Biol.* **290**, 161–173.
Collaborative Computational Project, Number 4 (1994). *Acta Cryst.* D**50**, 760–763.
Edwards, K. J., Barton, J. D., Rossjohn, J., Thorn, J. M., Taylor, G. L. & Ollis, D. L. (1996). *Arch. Biochem. Biophys.* **328**, 173–183.
Eklund, H., Nordstrom, B., Zeppezauer, E., Soderlund, G., Ohlsson, I., Boiwe, T., Soderberg, B. O., Tapia, O., Branden, C. I. & Akeson, A. (1976). *J. Mol. Biol.* **102**, 27–59.
John, J., Crennell, S. J., Hough, D. W., Danson, M. J. & Taylor, G. L. (1994). *Structure*, **2**, 385–393.
Leslie, A. G. W. (1992). *Jnt CCP4/ESF–EAMCB Newsl. Protein Crystallogr.*, **26**.
Matthews, B. W. (1968). *J. Mol. Biol.* **33**, 491–497.
Persson, B., Zigler, J. S. & Jornvall, H. (1994). *Eur. J. Biochem.* **226**, 15–22.
Rao, P. V., Krishna, C. M. & Zigler, J. S. (1992). *J. Biol. Chem.* **267**, 96–102.
Thorn, J. M., Barton, J. D., Dixon, N. E., Ollis, D. L. & Edwards, K. J. (1995). *J. Mol. Biol.* **249**, 785–799.
Tumminia, S. J., Rao, P. V., Zigler, J. S. & Russell, P. (1993). *Biochim. Biophys. Acta*, **1203**, 251–259.
Yagi, T. (1991). *J. Bioenerg. Biomembr.* **23**, 211–225.
Yokoyama, S., Hirota, H., Kigawa, T., Yabuki, T., Shirouzu, M., Terada, T., Ito, Y., Matsuo, Y., Kuroda, Y., Nishimura, Y., Kyogoku, Y., Miki, K., Masui, R. & Kuramitsu, S. (2000). *Nature Struct. Biol.* **7**(Suppl.), 943–945.